Computers and Structures, Volume 186, 1 July 2017, Pages 1 – 10
DOI: 10.1016/j.compstruc.2017.03.004

On the origin of computational model sensitivity, error, and uncertainty in threaded fasteners

G. M. Castelluccio[a,c], M. R. W. Brake[b,c]

[a] *School of Aerospace, Transportation and Manufacturing, Cranfield University, Cranfield, Bedfordshire, MK43 0AL, UK.*
[b] *William Marsh Rice University, 6100 Main st, Houston, TX, USA*
[c] *Previously at Component Science and Mechanics, Sandia National Laboratories, PO Box 5800 MS346, Albuquerque NM, USA*

Abstract

Modeling the mechanical response of components requires simplifications and idealizations that affect the fidelity of the results and introduce errors. Some errors correspond to the limited knowledge of intrinsic physical attributes while others are introduced by the modeling framework and mathematical approximations. This paper studies the dependence of the force-displacement response of threaded fasteners on modeling attributes such as geometry, material, and friction resistance using finite element simulations. A systematic comparison of $1D$, $2.5D$ or $3D$ computational models demonstrates the influence of model properties and the limitations of the methodologies. Finally, the paper discusses the sources of model inputs and model form errors for threaded fasteners.

Keywords: Threaded fasteners, Error quantification, Finite elements, Friction.

1. Introduction

Modeling the mechanical response of threaded fasteners often assumes simple $1D$ smooth geometry [1, 2] without considering the complex phenomena that take place in between threads. Similarly, reliability analyses of assemblies with multiple mechanical components usually rely on reduced order models that do not convey detailed geometric attributes, material properties, or frictional

*Corresponding author

effects. Instead, modeling large assemblies depends on equivalent constitutive behaviors of connectors (e.g., [3, 4]), which many times are assumed to be linear and reversible [5]. This modeling approach can introduce large errors that are unacceptable in the analysis of high consequence applications. Since the computational burden rapidly increases with increasing component size, there is a need not only to ascertain more accurate physics-based reduced order models, but also to quantify the model form error and the sources of variability [5].

Prior research on threaded fasteners investigated torsional tightening (or loosening) [6, 7], stress and strain distributions [8, 9], and fatigue life [10, 11], to mention a few of the most common aspects [12]. Nevertheless, few studies have focused on understanding and predicting the equivalent constitutive response of threaded fasteners. Furthermore, many of the existing studies employ simplified geometries (e.g., $2D$), linear elastic materials, and frictionless surfaces. Because most efforts focus on specific components, the conclusions from these publications cannot be generalized confidently to other scenarios. Therefore, there is a need to understand and generalize the relative impact of modeling assumptions and parameter errors on the force-displacement response of threaded fasteners.

A confident prediction of the mechanical response of threaded fastener needs to ascertain multiple sources of model uncertainty and sensitivity. Following the framework originated in the risk assessment community [13, 14], uncertainty (either epistemic or aleatory) in computational models may originate in numerical approximations, model inputs, and model form. Thus, this work investigates model input and form uncertainties in threaded fasteners by performing finite element simulations with various input parameters and model simplifications. We emphasize that we seek to understand the mechanisms that control the mechanical response of fasteners rather than reproducing certain experiments with simulations.

2. Sources of variability and error in modeling fasteners

The mechanical response of fasteners is determined by complex phenomena arising from the interaction of many physical bodies. To systematically study the fidelity of threaded fasteners models, we propose a taxonomy for the major sources of sensitivity, error, and uncertainty that affect the force-displacement response (Figure 1):

Geometry: Threaded fasteners are geometrically complex components with no axis of symmetry, which implies that only $3D$ models can yield exact results. Nevertheless, $2D$ simulations are still used to study threads (for example Ref. [15]). In addition, threads are manufactured with a wide range of quality, from inexpensive fasteners for disposable devises up to ultra-precise components for aerospace applications. As a result, geometrical attributes have a large variability among manufacturers, production batches, and applications; these may be mitigated with a statistical characterization of geometrical attributes.

Material: Manufacturing procedures have a notable effect on fastener material properties. Rolled threads present strong microstructural gradients [16] and texture while cut threads have discontinuous fibers with lower local strength [17, 18]. Even the manufacturing speed changes the microstucture and influences the mechanical response [16]. Thus, the identification of fasteners with their chemical composition or alloy grade conveys a large error that neglects residual stresses, microstructures, and defects. Multi-scale material models can mitigate these errors by explicitly incorporating sources of mesoscale variability [19, 20]. However, these strategies are computationally expensive, require a plethora of small-scale characterization, and represent a host of their own research challenges.

Mechanics: The mechanical response of fasteners is intimately related to the frictional interactions between the threads. These interactions are usually

captured with Coulomb friction models and a range of friction coefficients between 0 and 0.5 [21, 22]. Similarly, temperature changes or gradients, residual strains from installation, and loading direction also affect the response of fasteners. The coupling of these effects is an open problem and usually requires multi-scale and multi-physics approaches that are computationally and experimentally time-consuming.

Methodology: In addition to the intrinsic uncertainty of one particular fastener, computational models introduce acknowledged errors such as numerical rounding and spatial discretization errors, or unacknowledged errors such as coding mistakes. Recent efforts [23] have focused on identifying phases that introduce uncertainty and estimating the numerical error, but these sources of error are not the focus of this work.

Other sources of uncertainty may include loading history and environment assisted degradation (corrosion, radiation, etc) [24]. Although these aspects are beyond the scope of this work, as-produced and as-installed fasteners may degrade and alter their geometrical, material and mechanical attributes during the life of the component.

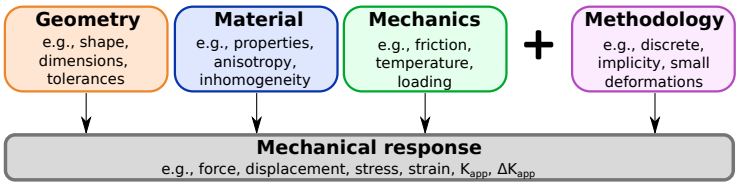

Figure 1: Most significant sources of sensitivity, error, and uncertainty in modeling the mechanical response of threaded fasteners.

A final comment pertains to the impact of the sources of sensitivity, error, and uncertainty on different quantities of interest, which are application-specific. In the case of threaded fasteners, the focus may be on the prediction the force-displacement response, torque-tension relation, the fracture and fatigue integrity, or the degradation during service, to mention a few. Since modeling uncertainty may affect these quantities in different manners or degree, the

propagation of errors should be carefully considered for each application.

This paper investigates the force-displacement response and stress and strain fields of threaded fasteners using $1D$, $2.5D$ or $3D$ finite element models with different geometrical attributes (sections 4.1, 4.2 and 4.3). These assessments also include sensitivity analysis of friction coefficients and material properties (elastic or elasto-plastic). Next, the effects of torsional installation strains are analyzed in section 4.4 and a comparison among models and experiments is presented in section 4.5. Finally, section 5 compares model inputs and model form errors, and discusses the results from various approaches.

3. Modeling approaches

This research investigates the relationships among a limited set of properties and models for *#0-40UNF* bolts [1] in Figure 2. In what follows the nomenclature of Figure 2 is used: a bolt consists of a head where load/torque is applied, a shank that connects the head with the threads, which engage with a substrate or a nut to form a stiff connector. Threads are characterized by number and pitch (e.g., 1/4-20 has a basic major diameter of 6.35mm and 20 threads per 25.4mm).

Regarding geometric variability, simulations employ $1D$ smooth models, $2.5D$ threaded models, and fully $3D$ threaded models, as shown in Figure 3. Here, $1D$ model refers to 3-dimensional smooth specimens with squared cross section and $2.5D$ model refers to 3-dimensional symmetric threaded models with one element into the thickness. In addition, $2.5D$ asymmetric models consider threads that are displaced by half the pitch at each side of the substrate and different substrate lengths (Figure 4). As previously shown by several researchers [25, 26, 27], the first five threads carry 90% of the load; thus, all cases include between four to five threads in contact between the bolt and the substrate.

The geometric characteristics of threads introduces difficulties in meshing $3D$ models with hexahedral elements, which are generally more accurate than tetrahedral finite elements. Therefore, $3D$ meshes are conformed by sections of

hexahedral and tetrahedral elements, with tied contact to make a continuous mesh (see Figure 3c). Hexahedral elements constitute most of the thread, where the highest stress and strain gradients occurs, while tetrahedral elements are employed for transitions with free surfaces and the inner core of the bolt.

Finite element simulations are conducted using the Sierra Finite Element software [28] with an implicit quasi-static solver. All meshes maintain similar element refinement to limit mesh size dependence, which does not strongly affect the force-displacement response [27]. Although a minor mesh dependence (about 10%) may exist on the peak stress and strain at the thread roots [8], this work assumes that the numeral uncertainty is negligible and focuses on the remaining sources of uncertainties. Certainly, the study by Rafatpanah [29] suggests that our mesh refinement is enough to yield mesh convergence of the shank stress.

The loading of the fastener consists of quasistatic normal displacement of the nodes on the top cross section of the bolt (displacement control). Torsional pre-strain are only considered in $3D$ models in section 4.4. The lateral and bottom boundaries of the substrate are constrained from displacing in any direction (see Figure 3). In $2.5D$ models, nodes are constrained from displacing in the out of plane direction (plane strain). Furthermore, friction is introduced by defining single contact between the bolt and the substrate, using an augmented Lagrange enforcement, which applies equal and opposite forces and iterates to achieve zero interpenetration [28] .

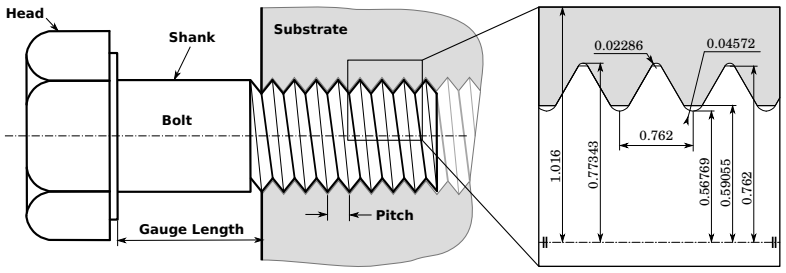

Figure 2: Nomenclature and geometrical details of the #0-40UNF bolt considered in simulations. Units in IS.

Models consider bolts made of A286 stainless steel while the substrate corre-

Table 1: Material properties for bolts (A286) and substrates (SS304L).

	A286	SS304L
Elastic modulus	200GPa	193GPa
Poisson ratio	0.28	0.28
Yield stress	827MPa	225 MPa
Hardening modulus	1100MPa	538MPa

sponded to 304L stainless steel, which are common in applications. Simulations employ two material models: isotropic linear elasticity or rate-independent linear hardening elasto-plasticity [30, 31]. Nominal material properties presented in Table 1 were adapted from [32]. Frictional effects are taken into account assuming Coulomb friction and various friction coefficients: $\mu = 0$, 0.15, 0.3, and 0.45 (typical of threaded connections [33]).

To compare actual forces rather than stresses, each simulation computes the total force on the nodes of the shank cross section (the top cross section of the bolt). Such a force is regularized by the ratio of the shank cross section in $3D$ model bolt and the shank cross section of the model considered, i.e.,

$$\text{Regularized force} = \text{Force}\frac{\text{Bolt cross-section in 3D models}}{\text{Bolt cross-section in current model}}. \tag{1}$$

Equation 1 is equivalent to computing the stress on the cross section of the bolt for the current model multiplied by the area of the bolt of interest. Similarly, the displacement applied to the top cross section of the bolt is regularized by the ratio of the total applied displacement in the $3D$ model (in number of pitches) and the gauge length in the $3D$ models (estimated as twice the thread pitch), i.e.,

$$\text{Regularized displacement} = \text{Applied displacement}\frac{\text{Displacement in 3D models}}{\text{Gauge length}}. \tag{2}$$

Thus, the regularized displacement represents the number of pitches that the head of the bolt has displaced.

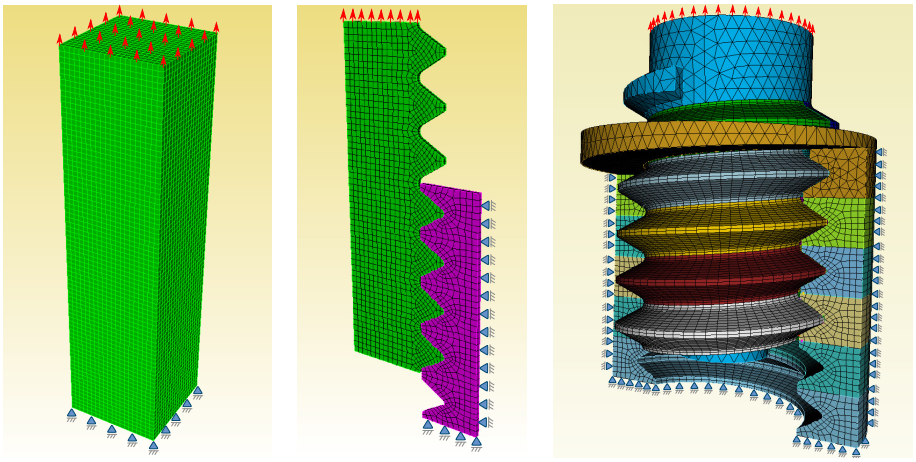

(a) 1D model. (b) 2.5D model. (c) Fully 3D model.

Figure 3: Examples of different finite element models.

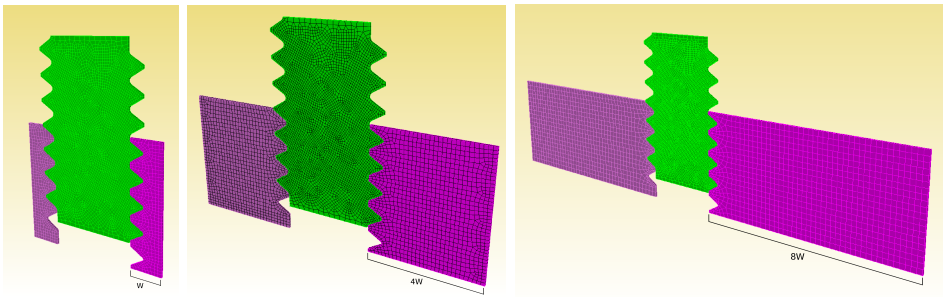

(a) Width=W. (b) Width=4W. (c) Width=8W.

Figure 4: 2.5D asymmetric models with different substrate lengths. Note the thread asymmetry.

4. Modeling results

4.1. Force-displacement from 2.5D asymmetric models

Figure 5 presents the regularized force-displacement response of threaded fasteners computed with 2.5D models for linear elastic (Left) and elasto-plastic (Right) materials; note the large difference on regularized force scales. Simulations consider multiple substrate lengths (referred to as W, 4W and 8W) and friction coefficients $\mu = 0$, 0.15, 0.3, and 0.45. The roughness of the curves corresponds to local instabilities that occur due to localized unloading.

For both material models, a higher friction coefficient limits the slip in threads and induces higher forces. Furthermore, larger substrates result in a lower compliance, and the responses for substrate lengths 4W and 8W show only minor differences, which suggests that these lengths may be enough to approximate a semi infinite substrate.

Although threads have complex geometrical features, linear elastic fasteners show an almost linear response (also found in Ref. [34]). This linearity suggests that geometrical attributes have a minor contribution to the force-displacement nonlinearity while material properties dominate the mechanical response. Indeed, the details of the thread geometry may not significantly affect the macroscopic response [35], especially for extended plastic deformation.

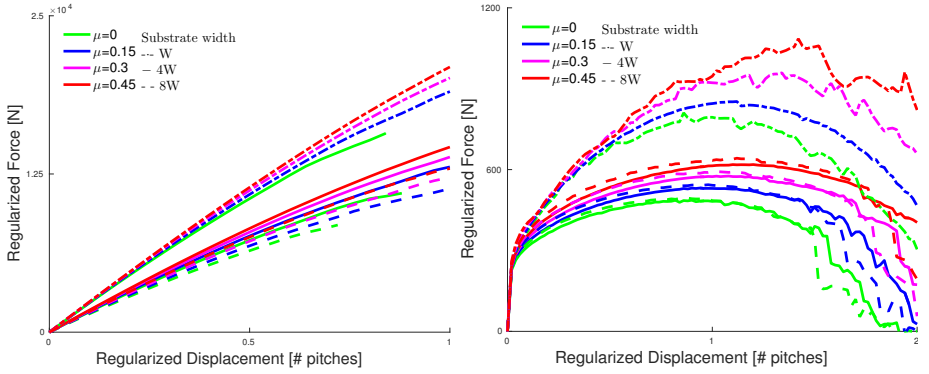

(a) Elastic materials. (b) Elasto-plastic materials.

Figure 5: Regularized force-displacement for $2.5D$ models for elastic (Left) and elasto-plastic (Right) materials, different substrate lengths (W, 4W and 8W), and friction coefficients ($\mu = 0$, 0.15, 0.3, and 0.45).

4.2. Force-displacement from $2.5D$ *and* $3D$ *models*

Figure 6 compares regularized force-displacement from $2.5D$ with $3D$ models using elastic (Left) and elasto-plastic (Right) materials and identical substrate lengths (W). Linear elastic materials result in an almost linear response with a different compliance for each model. Elasto-plastic models not only present a different compliance before yielding, but also yield at different load levels.

Indeed, $2.5D$ and $3D$ models seem to yield at two distinctly different force levels despite the regularization.

The response of $1D$ smooth specimen (Figure 3 a) is also presented in Figure 6 in black dotted lines. Contrary to strain calculations, the total displacement depends on the actual dimensions of the specimen. To regularize this magnitude for $1D$ models, we consider a gauge length of 40% of the total specimen length, which is chosen to match the elastic compliance of full $3D$ models shown in Figure 6a; the same regularization was employed for elasto-plastic models in Figure 6b.

The results show that $1D$ models can reproduce the axial force-displacement behavior of $3D$ models as long as they are scaled with an appropriate gauge length. Friction has a secondary effect on the response (also found by Ref. [36]), and their effects are smeared out by the gauge length. More importantly, a gauge length calibrated to match the elastic compliance results in adequate predictions for elasto-plastic models.

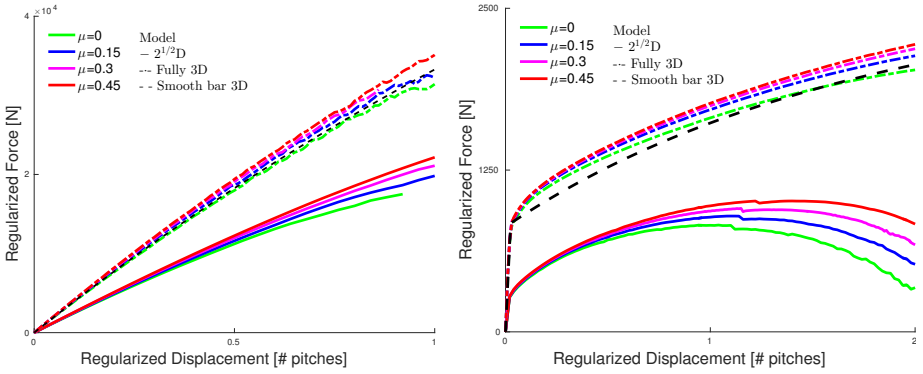

(a) Elastic materials. (b) Elasto-plastic materials.

Figure 6: Regularized force-displacement for $2.5D$ and $3D$ models for multiple friction coefficients. The results for $1D$ models (black dotted lines) are regularized to match the elastic compliance.

To investigate the discrepancy among $2.5D$ and $3D$ models, we simulated $2.5D$ models with a 220% and 440% increase in substrate thickness (note the out of plane dimension in Figure 7) and $3D$ wedge models (Figure 8). A 220% increase yields similar substrate cross sections between $2.5D$ and wedge models;

a 440% increase yields twice the cross-sections. In both cases, the displacement of the nodes normal to the sides of the models are restricted (these sides are not parallel in the case of wedges).

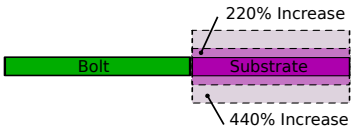

(a) Schematic top view of the bolt and substrates with different thickness.

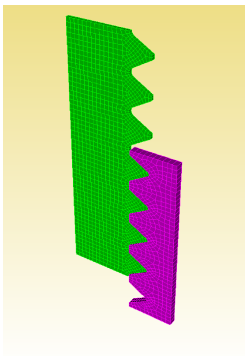

(b) 220% substrate thickness increase.

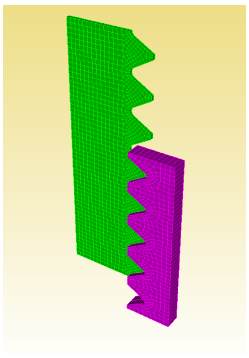

(c) 440% substrate thickness increase.

Figure 7: 2.5D models with different substrate thicknesses along the out of plane direction. (a) Top view comparison of substrate thickness. An increase in thickness results in equivalent (220%) substrate cross sections between 2.5D and wedge models or twice the cross sections (440%).

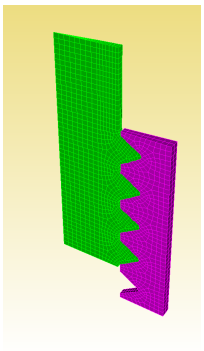

(a) 5° wedge.

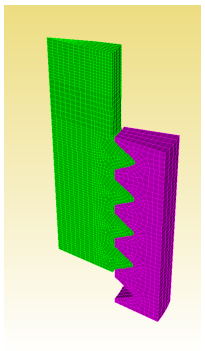

(b) 15° wedge.

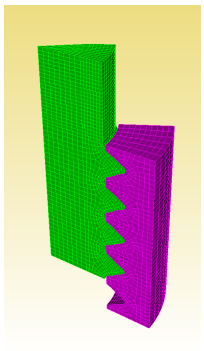

(c) 30° wedge.

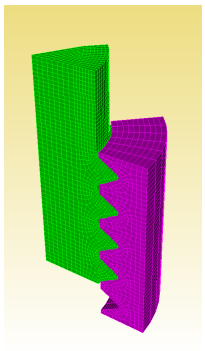

(d) 45° wedge.

Figure 8: 3D wedge models with different sweep angles. Compare the cross-sections from wedges to 2.5D models in Figure 7.

Figure 9 presents the regularized force-displacement from models with different substrate thicknesses and wedge angles. An increase in substrate thickness increases both the stiffness and yield force. The wedge sweep angle does not affect the yield force, but small wedge angles impose a higher constraint that

results in higher peak forces; these effects tend to saturate for wedges larger that 30°.

A major difference between $2.5D$ and $3D$ elasto-plastic models corresponds to the post-yield behavior. Wedge and full $3D$ models result in monotonic increase of the regularized force, but $2.5D$ models present a peak force (see Figure 6, for instance). Such a difference is, arguably, due to an intrinsic $3D$ effect of gradients in plastic deformation. Upon an increment in load, plastic deformation expands in the substrate and increases the deformation away from the thread. As the elastic/plastic boundary moves out from the thread, the change in the volume of resisting material along this boundary is different for $2.5D$ and $3D$ models.

Certainly, $2.5D$ models induce larger plastic deformation than $3D$ models due to their constant thickness in the out of plane direction. On the contrary, $3D$ models increase the resisting thickness away from the thread (i.e., the perimeter increases proportionally to the radius). Furthermore, thread cross sections do not remain planar upon loading in $3D$ models. A miscalculation of the resisting volume would also be corrected by employing $2D$ axisymmetric models, which seem to agree with $3D$ models [37]. A good agreement is expected given the low influence of the geometrical details (e.g., the helix, the transition between shank and thread) on the force-displacement response in our simulations.

4.3. Stress and strain field in $2.5D$ *and* $3D$ *models*

Figure 10 presents the equivalent plastic strain (*Eqps*) from $2.5D$ and $3D$ models with $\mu = 0.3$ at 30% and 70% of the maximum applied displacement. Significant differences are evident: $2.5D$ models show much higher strains within the substrate than $3D$ models. Secondly, the shank presents much higher deformation in $3D$ models. Both aspects are in agreement with a higher constraint imposed by the substrate in $3D$ models.

Similarly, Figure 11 presents the von Misses stress from $2.5D$ and $3D$ models at 30% and 70% of the maximum applied displacement (same as in Figure 10). The von Misses fields between $2.5D$ and $3D$ models are different, the latter

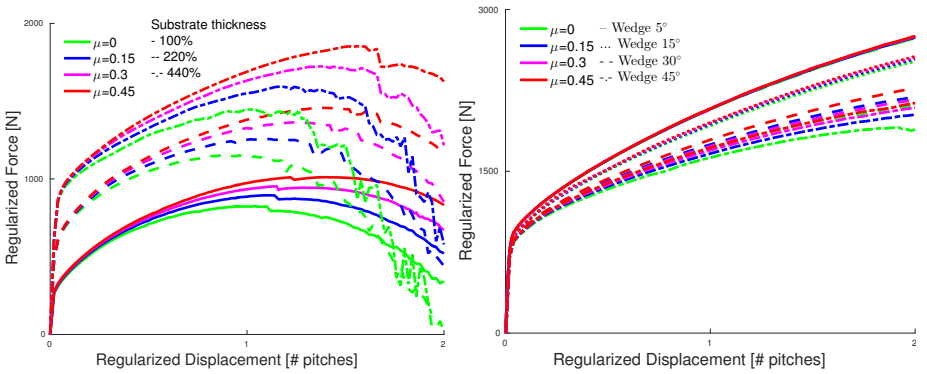

(a) Response of $2.5D$ models with multiple substrate thicknesses.

(b) Response of $3D$ wedge models with multiple angles.

Figure 9: Effects of the out-of-plane dimension on regularized force-displacement.

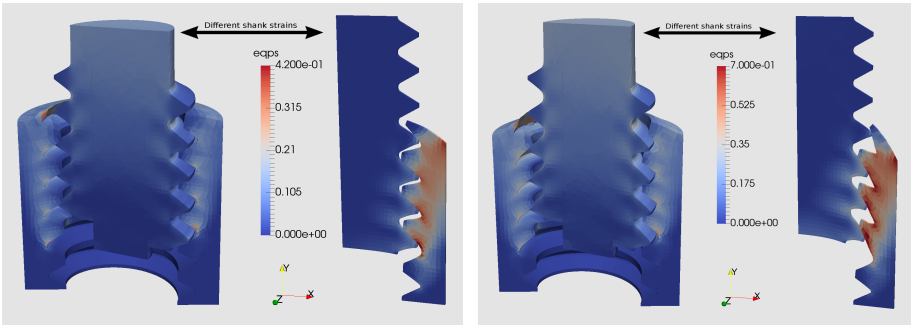

(a) (b)

Figure 10: Equivalent plastic strain fields for $2.5D$ and $3D$ models at 30% (Left) and 70% (Right) of the maximum applied displacement.

showing a much higher stress at the shank. The differences affect the expected failure mechanism of the fasteners: $3D$ models suggest that fasteners would fail due to plastic collapse of the shank while $2.5D$ models indicate that failure would occur due to the shear failure of the thread. Furthermore, the bottom thread is the most deformed in $2.5D$ models while the top threads are the most deformed in $3D$ models. Experiments for A286 bolts have shown that failure often occurs due to plastic collapse of the first engaged thread [38, 39, 40], as expected from the results of $3D$ models but not from $2.5D$ models.

A second consideration regards to the strain and stress fields in $2.5D$ models

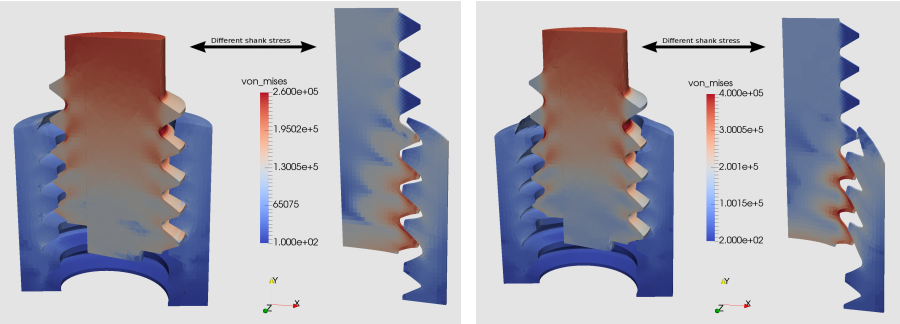

(a) (b)

Figure 11: von Misses stress fields for $2.5D$ and $3D$ models at 30% (Left) and 70% (Right) of the maximum applied displacement.

with larger substrates. If the thickness of the substrate controls the constraint on the bolt, then the stress and strain fields of wider substrates should resemble more closely those from $3D$ models. Figure 12 presents the *Eqps* (Left) and von Misses stress (Right) fields for $2.5D$ models with two different substrate widths at 30% of the maximum applied displacement. The comparison of Figure 12 (Left) with Figure 10 (Left) shows lower plastic deformation on the substrate and higher plastic strains on the shank with increasing substrate width, which indeed resembles $3D$ models. Regarding the von Misses stress field, Figure 12 (Right) depicts higher stresses on the shaft than Figure 11 (left). Furthermore, thicker substrates induce higher stresses and strains on the top threads, which is similar to $3D$ models.

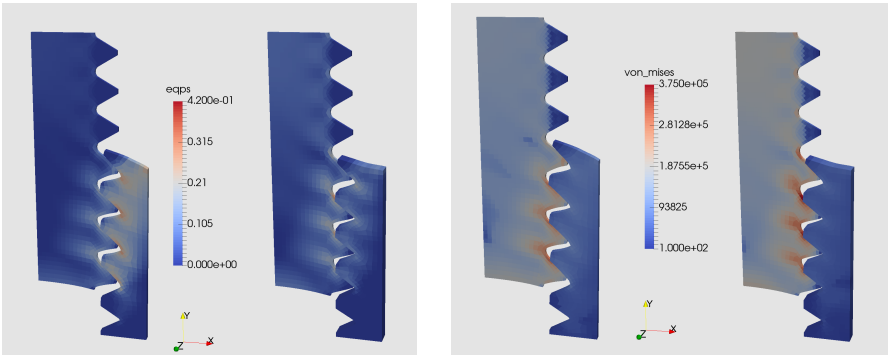

220% thicker substrate | 440% thicker substrate | 220% thicker substrate | 440% thicker substrate

Figure 12: Equivalent plastic strain (Left) and von Misses stress (Right) fields for 220% and 440% thicker substrates at 30% of the maximum applied displacement.

4.4. Torsional prestrains in 3D models

Another distinctive capability of $3D$ models is the consideration of torsional pre-strains from the installation of fasteners. Some efforts have focused on quantifying the correlation between installation torque and pre-load (e.g. [22, 7]), but not on the impact on the force-displacement evolution. To assess such effects, additional $3D$ simulations consider an initial rotation applied to the bolt. In this case, the top cross section of the bolt is initially constrained from displacing along the Y axis, which builds up stresses upon rotation.

Figure 13a presents the regularized force-displacement from $3D$ models with 15° bolt rotation and multiple friction coefficients. Similarly, Figure 13b presents the results for $\mu = 0.3$ and multiple rotation angles. The most significant effect of the torsion prior to pulling the bolt is an increase up to about 20% in the apparent yield level and a change in the apparent elastic stiffness. These effects are in agreement with the positive correlation between friction coefficient and torque-induced tension, [22].

In addition, Figure 14 presents the *Eqps* and von Mises stress for 30° rotation, $\mu = 0.3$ at 70% of the maximum applied displacement. Compared to Figures 10b and 11b, the stress and strains fields are equivalent with modest changes in the peak values (below 10%).

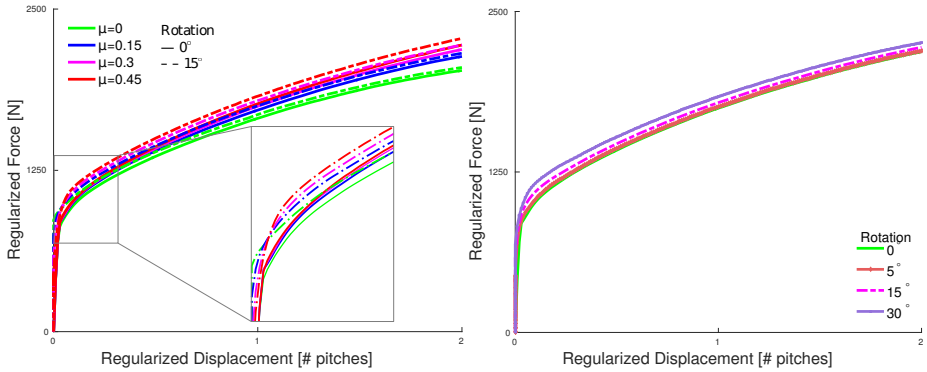

(a) 15° bolt rotation. (b) $\mu = 0.3$ friction coefficient.

Figure 13: Effect of torsional pre-strains in $3D$ models after rotating the bolt in regularized force-displacement. Pull-out simulations without rotation (0°) are also presented.

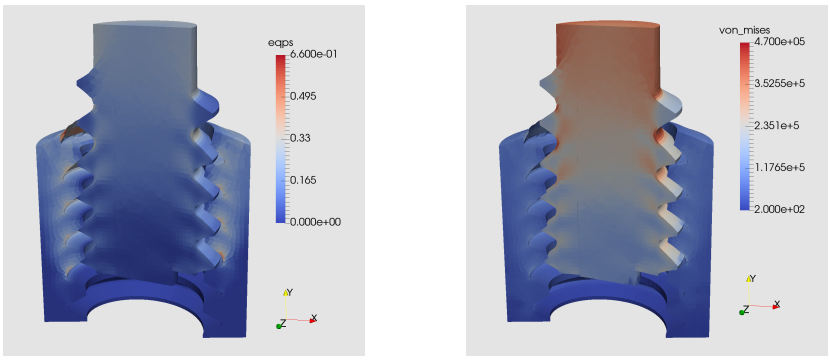

Figure 14: Equivalent plastic strain (Left) and von Misses stress (Right) for $3D$ models with 30° bolt rotation and $\mu = 0.3$ friction coefficient at 70% of the maximum applied displacement.

4.5. Comparison with experiments

To further understand the limitations of models, predictions from $3D$ models are compared to pull-out experiments for different bolts with A286 denomination. We consider four experimental pull-out tests:

- Exp-1 and Exp-2 from Ref. [41], which employed two *A286 #8-32, 5/8in* bolts using gauge lengths of 0.25in and 0.15in, respectively.
- Exp-3 from Ref. [42], which employed an *A286 #10-32, 5/8in* bolt with a gauge length of 0.2in.

- Exp-4 from Ref. [39], which employed an *A286 1/4-28, 2in* bolt with a 1.5in shank.

All experiments were performed under quasistatic loading without torsional pre-strains. The substrates were different among experiments but they all have a higher yield stress than A286 (e.g., 4140 steel); thus, we will assume an elastic substrate in simulations. Since the authors were not involved in performing these experiments, the modeling results in prior sections are blind and independent.

Current experimental methodologies carry such small errors in measuring forces and displacements (typically $<<$ 10%) that their impact on pull-out measurements can be neglected. However, models carry epistemic uncertainty (i.e., lack of knowledge) in the characterization of the real testing configuration. For example, the real gauge length up to the first engaged thread (see Figure 2), installation residual stresses/strains, bolt alignment, etc. Given the limited and systematic effect of friction coefficients on $3D$ models (see Figure 6 for instance), we argue that discrepancies among models and experiments are not controlled by friction, but dominated by testing conditions (rate, temperature), bolt dimensions, and material properties.

For comparison with experiments, a new set of $3D$ simulations was developed with an elastic substrate and no torsional pre-strain; results are presented in Figure 15a. Similarly to the methodology employed in Equation 1, forces were regularized by the ratio between model and test bolt cross sections. The regularization of the displacement is achieved by dividing by the gauge length (Exp-1, Exp-2, Exp-3) or the shank length(Exp-4), as shown by Equation 2. In simulations, the gauge length is twice the pitch length, which corresponds to the shank length in $3D$ models.

Figure 15a shows that the elastic compliance has a relatively wide range among experiments. The gauge length employed in the regularization of the displacement is partially responsible for this effect. A careful consideration of the resisting bolt length will likely improve the agreement, but such information is not available and is a source of error. In spite of these differences, models

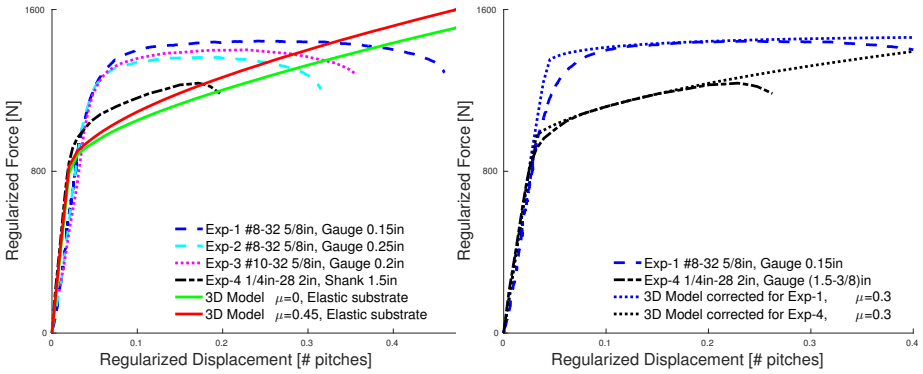

(a) As-produced material properties. (b) Strain hardened material properties.

Figure 15: Regularized force-displacement for $3D$ models and experiments.Left

approximately match the experimental elastic response with a regularization roughly estimated from experiments.

Exp-4 [39] presents a 30% lower regularized force at onset of plastic deformation (i.e., inelastic yield) than Exp-1, Exp-2 [41], Exp-3 [42]. Such a difference decreases with increasing displacement, and all the experiments present regularized peak forces within 15%. Furthermore, Exp-4 presents significantly more hardening than the other experiments, which are almost elastic-perfectly plastic. These differences suggest that the bolts from Exp-1, Exp-2, and Exp-3 have undergone additional work hardening during manufacturing, typical of small bolt size. The regularized yield force from models is slightly below that in the experiments from Exp-4 [39], while the degree of hardening is approximately equivalent and depends on the friction coefficient. Since the material properties for the models corresponds to as-rolled A286 steel, these differences are attributed to the microstructural changes and work hardening during the manufacturing process.

These arguments suggest that the lack of consideration of prior work hardening in the material properties controls the differences in force levels in Figure 15a. Therefore, an increase in the yield level and a decrease in hardening modulus (Table 2) would improve the matching to experiments. Similarly, the elastic compliance is controlled by the regularization length and differences in compli-

Table 2: Material properties and regularization length corrected for matching experiments. Substrates are considered elastic with a modulus of 200GPa.

	A286 Corrected for Exp-1	A286 Corrected for Exp-4
Elastic modulus	200GPa	193GPa
Poisson ratio	0.28	0.28
Yield stress	1310MPa	944MPa
Hardening modulus	269MPa	795MPa
Gauge length	1.55 pitch	1.55 pitch

ance between Exp-1 and Exp-4 may be attributed to an effective reduction in the gauge length due to 3/8in testing puck employed in Exp-4 [39, 40].

Figure 15b presents a new set of simulations with friction coefficient $\mu = 0.3$, gauge length of 1.55 pitches and material properties as presented in Table 2. Furthermore, the gauge length of Exp-4 is reduced by 3/8in to account for the testing puck. These results show good agreement among models and experiments, and suggest that material variability in $3D$ models can partially compensate for some uncertainty in friction coefficients, but not for geometrical changes in the gauge length or damage degradation.

The progressive reduction of the regularized force before failure is caused by the localization of plastic deformation and stable crack growth in the shank and first thread. Since these damage mechanisms are not explicitly considered, simulations result in monotonic force-displacement curves. Indeed, adjustments to the material properties to match the yield and hardening in experiments would not likely change such trends. Moreover, the non-monotonic behavior in $2.5D$ models is caused by the shear of the thread, which is not the failure mechanism found in experiments.

5. Discussion

Model form and model input errors coexist and they cannot always be distinguished or quantified. Thus, this section overviews the coupling of error sources.

Figures 5, 6, and 9 showed that various $2.5D$ simulations cannot reproduce the response of elasto-plastic $3D$ models, which are in better agreement with ex-

periments. Thus, model form errors in elasto-plastic $2.5D$ simulations dominate over model inputs such as friction coefficients, material properties, or geometric details. This behavior is attributed to an intrinsic miscalculation of the resisting volumes that controls the mechanical response, at least for bolts that fail due to plastic collapse of the shank or first thread rather than the shearing of the thread. Furthermore, this interpretation explains that $3D$ wedge or $2D$ axisymmetric models may provide reliable predictions even when some geometrical attributes are simplified.

Furthermore, simple $1D$ models can be *regularized* to reproduce $3D$ models closely (e.g., Figure 6), which supports standardized methodologies. In this case, model form error is small enough to be mitigated by modifying model inputs. Such a calibration (e.g., Equation 2) may be performed with elastic models that require low-computational effort, and later employed for elasto-plastic models.

Figures 5 and 6 demonstrate that elastic materials result in an almost linear behavior of the regularized force-displacement and suggest that geometric nonlinearities (e.g., the lack of cylindrical symmetry) induce a weak nonlinear response. On the contrary, elasto-plastic material properties impose a dominant nonlinear response. Hence, model input uncertainty is dominated by material properties, which control the force-displacement nonlinearity, and the gauge length, which controls the force-displacement elastic compliance.

Figures 6 and 9 indicate that friction effects and boundary conditions have a secondary but noticeable effect on the force-displacement response. This agrees with the minor impact of friction on load distribution found in Ref. [27]. More importantly, the effects of friction propagate consistently among various model inputs and forms, which yields confidence in extrapolating friction effects among different fasteners. In addition, torsional pre-strains affect the elastic compliance and the yield level (e.g., Figure 13), while the influence seems to be reduced upon further loading. These results suggest that uncertainty in torsional pre-strains may be mitigated by modifying model inputs.

Finally, Figure 15 shows that $3D$ models can reproduce the response of fasteners in experiments provided that the resisting length of the bolt is regularized

and that the material properties convey the manufacturing-induced microstructure. The error of these model inputs dominate over model form errors up to the maximum load. Upon softening after the peak force, model form increases due to the lack of consideration of plastic strain localization and stable crack growth. These aspects would require models that consider damage progression and self localization [43].

6. Conclusions

This work studied sources of computational modeling sensitivity, error, and uncertainty in the force-displacement response of threaded fasteners. The results showed that $2.5D$ finite element models have an intrinsic limitation for representing the force-displacement response of threaded fasteners that fail due to plastic collapse. Indeed, simpler $1D$ smooth specimens can be scaled to match more closely the results from $3D$ models and experiments up to the peak load with the appropriate model inputs.

In $3D$ models, material properties and the gauge length affect the most the nonlinear response and elastic compliance of fasteners, respectively. The influence of friction propagates consistently among various model forms and inputs. Furthermore, by comparing computational models and experiments we argued that manufacturing processes introduce ranges of properties within the fasteners that affect mostly the yield force and hardening modulus. Future work will seek to model the effect of microstructural variability and material property gradients on fastener response.

References

[1] ASME - STANDARDS B1.1:2003 - Unified Inch Screw Threads, (UN and UNR Thread Form).

[2] J. H. Bickford, An introduction to the design and behavior of bolted joints, Marcel Dekker, New York, 1995.

[3] J. Abad, J. Franco, R. Celorrio, L. Lezun, Design of experiments and energy dissipation analysis for a contact mechanics 3d model of frictional bolted lap joints, Advances in Engineering Software 45 (1) (2012) 42 – 53.

[4] M. Iranzad, H. Ahmadian, Identification of nonlinear bolted lap joint models, Computers & Structures 9697 (2012) 1 – 8.

[5] J. L. Dohner, White paper: On the development of methodologies for constructing predictive models of structures with joints and interfaces. SAND2001-0003P, Tech. rep., Sandia National Laboratories, Albuquerque, NM (2001).

[6] S. Izumi, T. Yokoyama, A. Iwasaki, S. Sakai, Three-dimensional finite element analysis of tightening and loosening mechanism of threaded fastener, Engineering Failure Analysis 12 (4) (2005) 604 – 615.

[7] Q. Yu, H. Zhou, L. Wang, Finite element analysis of relationship between tightening torque and initial load of bolted connections, Advances in Mechanical Engineering 7 (5) (2015) 1–8.

[8] J. W. Hobbs, R. L. Burguete, E. A. Patterson, Investigation into the effect of the nut thread run-out on the stress distribution in a bolt using the finite element method, Journal of Mechanical Design 125 (3) (2003) 527 – 532.

[9] Q. Yu, H. Zhou, Finite element study on pre-tightening process of threaded connection and failure analysis for pressure vessel, Procedia Engineering 130 (2015) 1385 – 1396.

[10] M. Zhang, Y. Jiang, C.-H. Lee, Finite Element Modeling of Self-Loosening of Bolted Joints, Journal of Mechanical Design (2006) 218 – 226.

[11] J. Williams, R. Anley, D. Nash, T. Gray, Analysis of externally loaded bolted joints: Analytical, computational and experimental study, International Journal of Pressure Vessels and Piping 86 (7) (2009) 420 – 427.

[12] J. Mackerle, Finite element analysis of fastening and joining: A bibliography (19902002), International Journal of Pressure Vessels and Piping 80 (4) (2003) 253 – 271.

[13] C. Soize, Generalized probabilistic approach of uncertainties in computational dynamics using random matrices and polynomial chaos decompositions, International Journal for Numerical Methods in Engineering 81 (8) (2010) 939 – 970.

[14] C. J. Roy, W. L. Oberkampf, A comprehensive framework for verification, validation, and uncertainty quantification in scientific computing, Computer Methods in Applied Mechanics and Engineering 200 (2528) (2011) 2131 – 2144.

[15] N. L. Pedersen, Optimization of bolt thread stress concentrations, Archive of Applied Mechanics 83 (1) (2013) 1 – 14.

[16] J. A. Mohandesi, M. A. Rafiee, O. Maffi, P. Saffarzadeh, Dependence of the yield and fatigue strength of the thread rolled mild steel on dislocation density, Journal of Manufacturing Science and Engineering 129 (1) (2006) 216 – 222.

[17] J. P. Domblesky, F. Feng, A parametric study of process parameters in external thread rolling, Journal of Materials Processing Technology 121 (23) (2002) 341 – 349.

[18] H. Fransplass, M. Langseth, O. Hopperstad, Tensile behaviour of threaded steel fasteners at elevated rates of strain, International Journal of Mechanical Sciences 53 (11) (2011) 946 – 957.

[19] G. M. Castelluccio, D. L. McDowell, Mesoscale modeling of microstructurally small fatigue cracks in metallic polycrystals, Materials Science and Engineering: A 598 (2014) 34 – 55.

[20] J. E. Bishop, J. M. Emery, C. C. Battaile, D. J. Littlewood, A. J. Baines, Direct numerical simulations in solid mechanics for quantifying the

macroscale effects of microstructure and material model-form error, JOM 68 (5) (2016) 1427 – 1445.

[21] J. Cornwell, Some observations on friction in screw threads, Wear 67 (3) (1981) 329 – 339.

[22] D. Croccolo, M. D. Agostinis, N. Vincenzi, Failure analysis of bolted joints: Effect of friction coefficients in torquepreloading relationship, Engineering Failure Analysis 18 (1) (2011) 364 – 373.

[23] W. L. Oberkampf, S. M. DeLand, B. M. Rutherford, K. V. Diegert, K. F. Alvin, Error and uncertainty in modeling and simulation, Reliability Engineering & System Safety 75 (3) (2002) 333 – 357.

[24] L. Solazzi, R. Scalmana, M. Gelfi, G. M. La Vecchia, Effect of different corrosion levels on the mechanical behavior and failure of threaded elements, Journal of Failure Analysis and Prevention 12 (5) (2012) 541 – 549.

[25] D. L. Miller, K. M. Marshek, M. R. Naji, Determination of load distribution in a threaded connection, Mechanism and Machine Theory 18 (6) (1983) 421 – 430.

[26] W. Wang, K. Marshek, Determination of load distribution in a threaded connector with yielding threads, Mechanism and Machine Theory 31 (2) (1996) 229 – 244.

[27] J.-J. Chen, Y.-S. Shih, A study of the helical effect on the thread connection by three dimensional finite element analysis, Nuclear Engineering and Design 191 (2) (1999) 109 – 116.

[28] Sierra Mechanics, Finite Element Software, version 4.38.1 (2014).

[29] R. M. Rafatpanah, Finite element analysis of a three-dimensional threaded structural fastener, Master's thesis, Rensselaer Polytechnic Institute (2013).

[30] Sierra/SM Development Team, Sierra/SM 4.32 verification tests manual, SAND Report 2014-3257, Sandia National Laboratories, Albuquerque, NM and Livermore, CA (2014).

[31] R. Hill, The Mathematical theory of plasticity, by R. Hill,..., the Clarendon press, Oxford, 1950.

[32] www.MatWeb.com (Last access: April 2016).

[33] S. A. Nassar, H. El-Khiamy, G. C. Barber, Q. Zou, T. S. Sun, An experimental study of bearing and thread friction in fasteners, Journal of Tribology 127 (2) (2005) 263 – 272.

[34] D. J. Segalman, M. J. Starr, Modeling of Threaded Joints Using Anisotropic Elastic Continua, Journal of Applied Mechanics 74 (3) (2006) 575 – 585.

[35] G. P. O'Hara, Elastic comparison of four thread forms. ARCCB-TR-98001, Tech. rep., US Army Armament Research, Development and Engineering Center, Watervliet NY (1998).

[36] Z. Hua, Analysis of the load distribution in a bolt-nut connector, Computers & Structures 53 (6) (1994) 1465 – 1472.

[37] L. Adam, A. Daidié, B. Castanié, E. Bonhomme, Application of high-performance computing to a bolt static tensile test, International Journal on Interactive Design and Manufacturing (IJIDeM) 6 (3) (2012) 195 – 203.

[38] P. M. Wade, Characterization of high-strength bolt behavior in bolted moment connections - NCSU digital repository, Master's thesis, North Carolina State Universtity (2006).

[39] J. T. Whittaker, D. P. Hess, Ductility of titanium alloy and stainless steel aerospace fasteners, Journal of Failure Analysis and Prevention 15 (5) (2015) 571 – 575.

[40] J. T. Whittaker, Ductility and use of titanium alloy and stainless steel aerospace fast, Master's thesis, University of South Florida (2015).

[41] K. J. Moore, M. R. W. Brake, A reduced order model of force displacement curves for the failure of mechanical bolts in tension. SAND2015-10871, Tech. rep., Sandia National Laboratories, Albuquerque, NM (2015).

[42] L. Sangwook, M. Sam, K. J. S., L. Kenneth, Experimental results of single screw mechanical tests: a follow-up to SAND2005-6036. SAND2006-3751, Tech. rep., Sandia National Laboratories, Albuquerque, NM (2006).

[43] R. Liao, Y. Sun, J. Liu, W. Zhang, Applicability of damage models for failure analysis of threaded bolts, Engineering Fracture Mechanics 78 (3) (2011) 514 – 524.